Overall Stability of Welded Q460GJ Steel Box Columns: Experimental Study and Numerical Simulations

Zhou Xiong, Kang Shao Bo, Yang Bo

Abstract—To date, high-performance structural steel has been widely used for columns in construction practices due to its significant advantages over conventional steel. However, the same design approach with conventional steel columns is still adopted in the design of high-performance steel columns. As a result, its superior properties cannot be fully considered in design. This paper conducts a test and finite element analysis on the overall stability behaviour of welded Q460GJ steel box columns. In the test, four steel columns with different slenderness and width-to-thickness ratio were compressed under an axial compression testing machine. And finite element models were established in which material nonlinearity and residual stress distributions of test columns were included. Then, comparisons were made between test results and finite element result, it showed that finite element analysis results are agree well with the test result. It means that the test and finite element model are reliable. Then, we compared the test result with the design value calculated by current code, the result showed that Q460GJ steel box columns have the higher overall buckling capacity than the design value. It is necessary to update the design curves for Q460GJ steel columns so that the overall stability capacity of Q460GJ box columns can be designed appropriately.

Keywords—Axial compression, Finite element analysis, Overall stability, Q460GJ steel, Welded box columns

I. INTRODUCTION

COMPARED with traditional steels, HPS has the characteristic of high strength, excellent plasticity, impact toughness, lamellar tearing resistance and well welding property with low carbon equivalent [1], such as GJ series steel in China [2], HPS series in the United States [3], BHS series in Japan [4] and S460, S490 in Europe [5]. Because of many excellent properties, it was widely applied in engineering structure and brought considerable economic benefit. Such as the Berlin, Star City in Sydney, etc. Their application brought huge economic and social effects. But, the current design standard may not be appropriate for these new-type kinds of steels. Since studies began in 1960s, researchers in the United States and Japan have started research on HPS [6]-[8]. In Europe, the fatigue characterization and structural stability of HPS was studied deeply. And the design principles for HPS

Zhou Xiong is with Key Laboratory of New Technology for Construction of Cities in Mountain Area, Ministry of Education and School of Civil Engineering, Chongqing University, CO 400045, China (phone: 86-18883701962; e-mail: zhxiongs@163.com).

Kang Shao Bo and Yang Bo are with Key Laboratory of New Technology for Construction of Cities in Mountain Area, Ministry of Education and School of Civil Engineering, Chongqing University, CO 400045, China.

was accepted into Eurocode [9]. Compared with developed countries, Chinese researches only then just started the HPS research. Starting in 2006, Shi et al. [10] studied the basic mechanical properties of Q690 and Q460. Thereafter the stability behaviour of high-strength steel compression components was studied. Their results showed the whole stability coefficient φ is improved evidently compared with ordinary mild steel [10]-[12]. Wang et al. [13] have come to the similar conclusion. While, Yang et al. [14], [15] studied the lateral torsional buckling of Q460GJ structural steel beams. It shows that the design methods employed from GB 50017-2003 [16] and ANSI/AISC360-10 [17] may be not conservative for global stability of welded Q460GJ structural steel beams. In order to establish a mature design principle for HPS structures, there still leaves lots of researches to be conducted.

As an important part of the series of HPS research, four 460GJ box section columns with different width-thickness ratio and normalized slenderness were researched in this paper. The buckling model was controlled by the nominal width-thickness ratio restriction based on GB 50017-2003, Eurocode 3 and ANSI/AISC 360-10 [9], [16], [17]. In addition, a finite element model was established to predict the buckling behaviour of Q460GJ box columns. Then the test result were cross-checked with FEM result to evaluate the reliability of this research. Finally, these results were provide the foundation for Q460GJ box section design.

II. EXPERIMENTAL PROGRAMME

A. Specimen Design

Four columns fabricated of high-performance Q460GJ steel and designed with different width-thickness ratio and normalised slendernesses, were tested under axial compression. The nominal flange and web thickness was 12 mm or 25 mm. And the slenderness of columns ranged from 90 to 120. Fig. 1 shows the definition of symbols for a column section. Table I list the dimensions of steel columns. For all columns, the cross dimensions and slendernesses was defined based on the constraints of testing machine. Also, they were designed to make sure the columns were failed in global buckling. According to GB 50017-2003 [16], as expressed in (1). The limits value for local buckling avoided was also satisfied the requirements in Eurocode 3 [9] and ANSI/AISC 360-10 [17].

$$b'/t \le 40\sqrt{\frac{235}{f_y}} \qquad (1)$$

World Academy of Science, Engineering and Technology
International Journal of Structural and Construction Engineering
Vol:11, No:11, 2017

where b' and t are the net width and thickness of column walls, respectively, and f_y is the yield strength of steel plates.
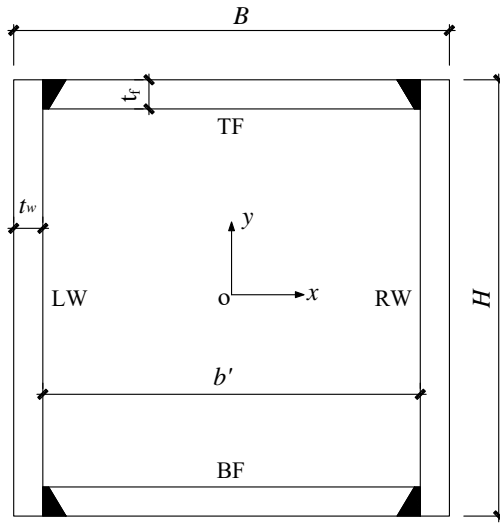

Fig. 1 Definition of symbols for a column section

B. Test Configuration

Fig. 2 shows the test configuration. Two reinforce plates with a thickness of 30 mm were welded to end of columns to prevent premature end failure. Besides, the simply supported boundary conditions was formed at the ends of column and the column could rotate freely about y-axis. During testing, transducers labelled DH were used to measure horizontal displacement of the column. Similarly, the vertical deformation was measured by transducers labelled as DV. Inclinometer Q1 was mounted at the testing machine to monitor its rotation. Another two inclinometers, Q2 and Q3, were located at both ends of column to measure angles of rotation. As shown in Fig. 3, 11 strain gauges were used to measure the strain course and distributions at the mid-length cross section.

C. Initial Imperfection.

Initial imperfection, including geometric imperfection (initial bending and loading eccentricity) and residual stress were measured before compression testing. Fig. 4 illustrates the measuring-point arrangement for initial bending. Three points were set along the quartile of column. And the measuring result achieved by measuring-point were marked as v_1, v_2 and v_3, correspondingly. Table II lists the average of deformations at the measured points. The horizontal distance between the column centre line and the centre of rotation at the top and the button of the column was measured as loading eccentricity labelled as e_t and e_b. Table II lists the measured result. At last, the geometric imperfection was calculated by (2):

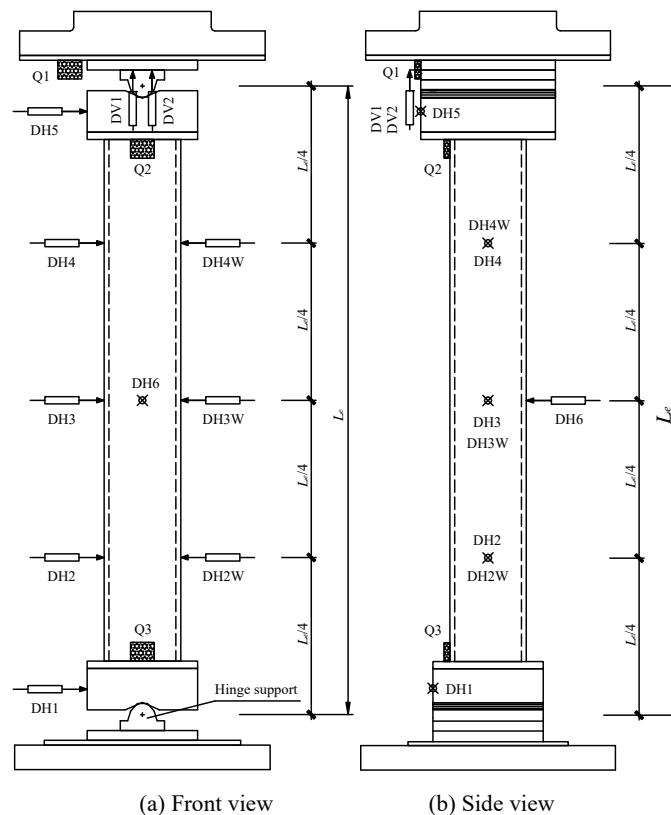$$e = \left(e_t + e_b\right)/2 + v_{\max} \qquad (2)$$

(a) Front view   (b) Side view

Fig. 2 Test setup for steel columns under axial compression

World Academy of Science, Engineering and Technology
International Journal of Structural and Construction Engineering
Vol:11, No:11, 2017

TABLE I
MEASURED DIMENSIONS OF STEEL COLUMNS

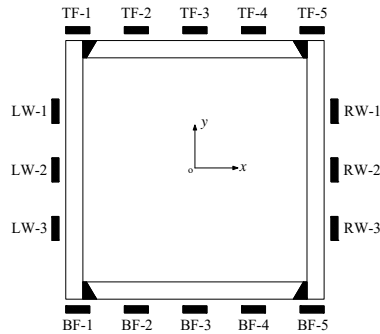| Specimen	H (mm)	t_w (mm)	B (mm)	t_f (mm)	b'/t	i_y (mm)	L (mm)	L_e (mm)	λ
B-120-12	120.37	12.37	120.21	12.23	7.8	44.39	3115.00	3493.00	110
B-168-12	168.51	12.43	168.04	12.45	11.5	63.74	3733.50	4111.50	90
B-175-25	176.18	25.87	174.42	25.53	4.8	61.75	4945.60	5323.60	120
B-200-25	201.96	25.62	197.97	25.42	6.8	71.41	4776.50	5154.50	100

Fig. 3 Layout of strain gauges

The residual stress was tested from sectioning method. It was similar to I-sections [13]. The test result would be employed for numerical simulations of steel box columns under axial compression.
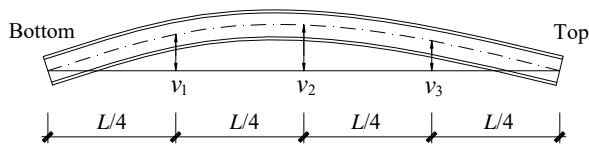

Fig. 4 Measurement of geometric imperfections

TABLE II
INITIAL GEOMETRIC IMPERFECTION IN BUCKLING PLANE

Specimen	Initial bending (mm)				Loading eccentricity (mm)		e (mm)
	v_1	v_2	v_3	v_{max}	e_b	e_t	
B-120-12	2.34	2.20	2.16	2.34	0.50	1.75	3.45
B-168-12	0.42	1.08	1.19	1.19	2.00	5.25	4.82
B-175-25	2.74	2.33	2.74	2.74	3.00	2.25	5.37
B-200-25	3.03	3.42	2.57	3.42	0.00	3.75	5.23

III. TEST RESULTS AND DISCUSSIONS

A. Material Properties

Three steel plate were used to manufacture the columns. For each plate, three tension coupons were extracted to the tension test, and the results were combined by an averaging. Table III lists the yield and ultimate strengths of each steel plates.

Besides yield and ultimate strengths, elongations were also obtained by strain gauges and an extensometer. Yield and ultimate strains were determined, correspondingly.

B. Buckling Behaviour

Fig. 5 shows the strain course at cross section of B-120-12, as cross section strain distribution of the rest specimens are similar. It can be observed that the applied load increased almost linearly with increasing strain at the initial stage. Before attaining the load capacity, nonlinear behaviour developed in the columns. Thereafter, global buckling of columns decreased the load gradually. It reveals that the buckling behaviour is a typical instability phenomenon of extreme point type. The curve met a sudden change shortly after the load undergoing the descent part. The main reason, after analysis, was that the cylinder hinge encounter a sudden slip. The horizontal displacement of cylinder hinge was listed in Table IV. The displacement before and after the ultimate load are add up to the total slip. It indicates that the slip of hinge has negligible effect on the capacity of columns, since its majority displacement occurred during the descent stage or it has a negligible displacement before reached the ultimate load. The relation curve about axial load and mid-length horizontal displacement was illustrated in Fig. 5. It also manifested characteristics of extreme point instability.
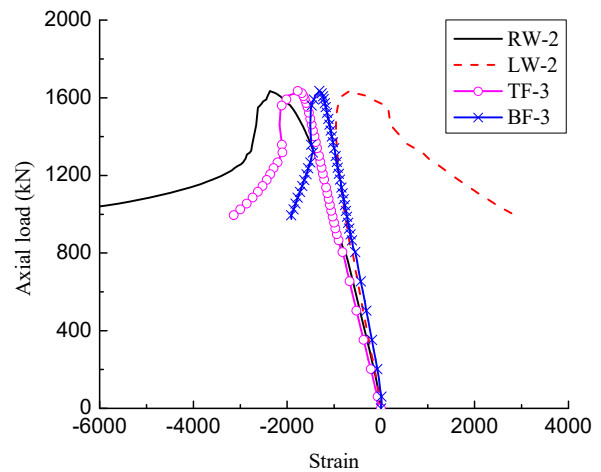

Fig. 5 Load-strain curves of steel column B-120-12

TABLE III
MATERIAL PROPERTIES OF STEEL PLATES

Plate number	Thickness (mm)	Elastic modulus (GPa)	Yield strength (MPa)	Yield strain	Ultimate strength	Ultimate strain	Remark
T12	12	209	571	0.019	678	0.094	All walls
T25-1	25	211	485	0.013	628	0.114	LW/RW
T25-2	25	208	424	0.023	563	0.140	TF/BF

World Academy of Science, Engineering and Technology
International Journal of Structural and Construction Engineering
Vol:11, No:11, 2017

TABLE IV
CYLINDER HINGE HORIZONTAL DISPLACEMENT

Specimen	Before ultimate load (mm)		After ultimate load (mm)	
	Top	Bottom	Top	Bottom
B-120-12	1.06	0.93	3.46	3.93
B-168-12	1.78	0.81	4.29	0.53
B-175-25	2.10	1.52	11.33	0.66
B-200-25	3.63	1.25	9.55	3.19

C. Test Strength and Comparison with Design Curves

Table V summarizes the ultimate loads, buckling factor and the normalized slenderness λ_n. The calculation formal for φ and λ_n are shown as (3) and (4). For each columns, the load capacity was calculated based on the current code GB500117-2003 [13]. The ratio of experimental to calculated load capacity varied from 1.21 to 1.42. It reveals that the design capacity obtained from GB50017-2003 [16] is generally conservative, even the eccentricity load surpassed Le/1000.
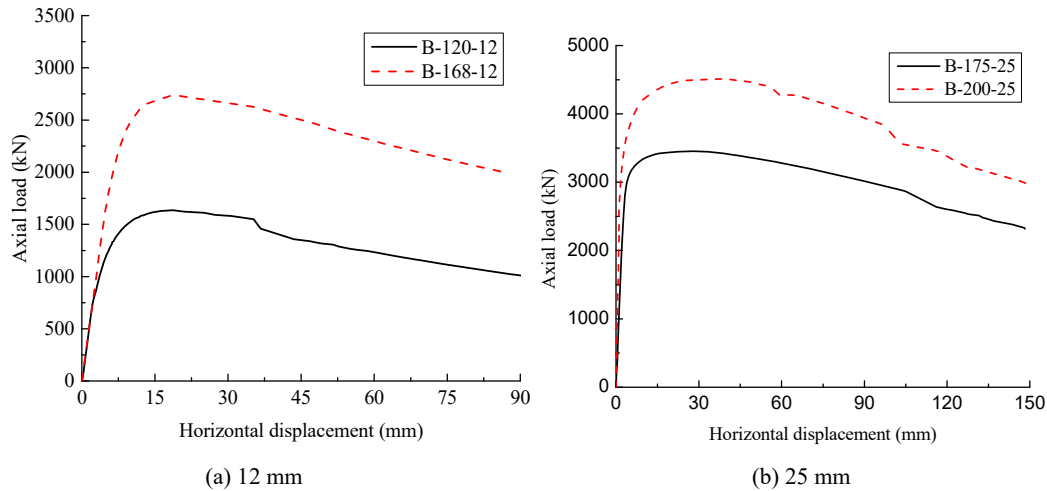

(a) 12 mm (b) 25 mm

Fig. 6 Axial load-horizontal displacement curves of steel columns

TABLE V
LOAD CAPACITY AND BUCKLING FACTOR

Specimen	Load capacity P_u (kN)	Yield strength P_y (kN)	Buckling factor φ	Normalized slenderness λ_n	Load capacity P_{uG} in GB50017-2003 (kN)	P_u/P_{uG}
B-120-12	1635.5	3033.8	0.54	1.29	1149.54	1.42
B-168-12	2739.9	4428.1	0.62	1.05	2097.64	1.31
B-175-25	3452.9	7077.0	0.49	1.30	2656.28	1.30
B-200-25	4511.4	8181.9	0.55	1.09	3734.31	1.21

$$\varphi = \frac{P_u}{A f_y} \qquad (3)$$

$$\lambda_n = \frac{\lambda_y}{\pi}\sqrt{f_y/E}$$
$$\lambda_y = \lambda\sqrt{235/f_y} \qquad (4)$$

in which E is the modulus of elasticity.

IV. FINITE ELEMENT ANALYSES

A. Finite Element Model

The non-linear finite element analyses containing imperfections were performed in the ABAQUS. C3D8R element with reduced integration was employed for steel columns. The mesh size applied for finite model was determined by two principal factors: (1) the residual stress pattern should simulated accurately; (2) the calculating result was almost fixed in the case of a further subdivided. Fig. 7

shows the residual stress distribution on one section. It was measured through sectioning method. The bilinear material model was employed for the material property introduced into the model. Shown in the Fig. 6, the columns have failed before the strain reached yield level, and thus it is appropriate for that. The corresponding parameters in the model were based on coupon tests.
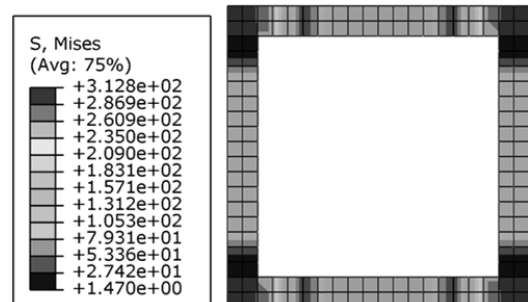

Fig. 7 Residual stresses in steel column B-120-12

World Academy of Science, Engineering and Technology
International Journal of Structural and Construction Engineering
Vol:11, No:11, 2017

TABLE VI
COMPARISONS BETWEEN LOAD CAPACITIES OF STEEL COLUMNS

Specimen	Test value P_u (kN)	Numerical result P_e (kN)	$\dfrac{P_e}{P_u}$
B-120-12	1635.5	1603.1	0.980
B-168-12	2739.9	2779.8	1.015
B-175-25	3452.9	3241.6	0.939
B-200-25	4511.4	4601.8	1.020
Mean ratio			0.989

B. Validation of the Finite Element Model

The buckling capacity predicted by FE analyses was listed in Table VI. It showed that the numerical result are very close to the experimental results. In addition, Fig. 8 illustrates that the test and numerical load-lateral displacement curves are coincided well even the ultimate capacity reached. These results demonstrate that the finite element analysis and the experiment can be proved mutually.
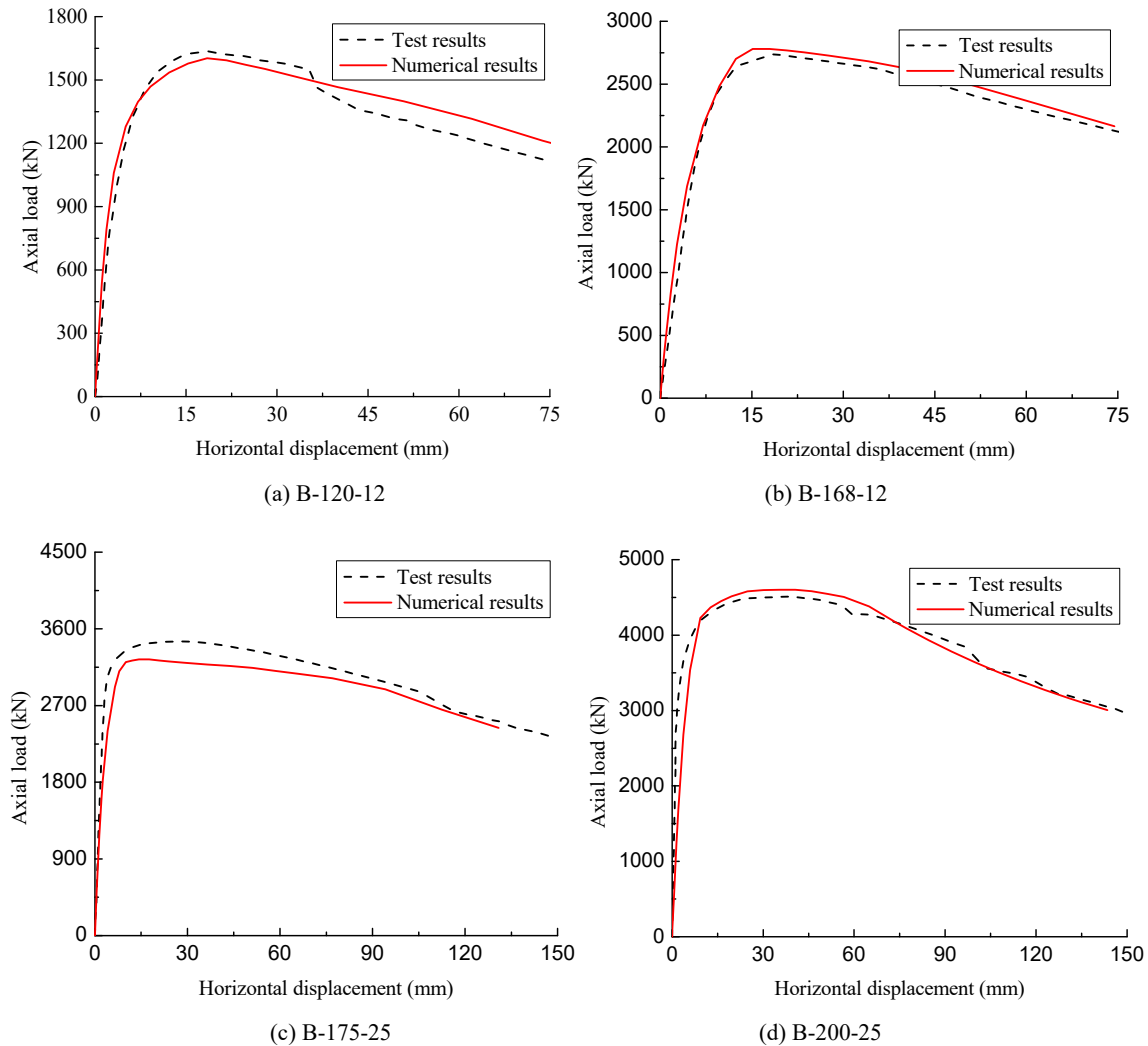

(a) B-120-12

(b) B-168-12

(c) B-175-25

(d) B-200-25

Fig. 8 Comparisons between experimental and numerical results

V. DISCUSS AND CONCLUSIONS

Based on the Table IV, the capacity of Q460GJ box columns is far higher than the design load. Then, comparisons were made between load capacities obtained from experimental tests and calculated by curve b in GB50017-2003 [16] and Eurocode 3 [9], and the capacity also calculated by AISC 360-10 [17]. Fig. 9 shows the results. The ratio of experimental to calculated load varied from 1.01 to 1.24. It can be considered that reasonable results could be obtained when the design curve b in GB50017-2003 and Eurocode 3 were used for global buckling design of welded Q460GJ steel box columns. And a similar conclusion was also obtained when the design approach in AISC 360-10 [17] was used. Based on numerical results and test results of box columns under axial compression and the, curve 'b' in GB50017-2003 [16] and Eurocode 3 [9] is recommended for global buckling design of Q460GJ steel box columns under axial compression. And AISC 360-10 is also appropriate for Q460GJ steel box columns. This conclusion was reliable under the conditions of the experiment. The present study only focused on four columns of Q460GJ steel, different performance can be expected when the columns with different width-thickness ratio and slenderness. Therefore, further experimental tests and numerical simulations on steel

World Academy of Science, Engineering and Technology
International Journal of Structural and Construction Engineering
Vol:11, No:11, 2017

column under combined axial load should be conduct in order to fully quantify the advantages of GJ steel columns over conventional members in buckling behaviour.
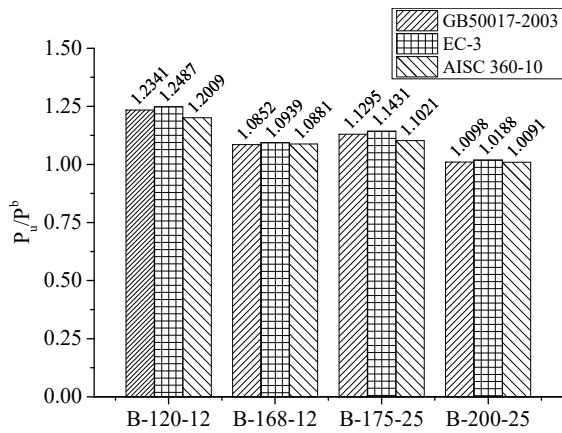

Fig. 9 The ratio of test load and design capacity by different codes

REFERENCES

[1] Bjorhovde R. Development and use of high performance steel. *Journal of Constructional Steel Research*, vol.60, pp.393-400, 2004.

[2] GB/T 19879-2005 Steel Plates for Building Structure. Beijing: Quality inspection of China press: 2005 (in Chinese).

[3] Raoul J. Use and application of high-performance steels for steel structures. *Iabse*, 2005.

[4] Miki C, Ichikawa A, Kusunoki T, et al. Proposal of New High Performance Steels for Bridges (BHS500, BHS700). *Journal of Structural Mechanics and Earthquake Engineering*, vol.738, pp.1-10, 2003.

[5] EN 1993-1-10. Design of Steel Structures. Part 1-10: Material Toughness and Through-Thickness Properties.2005.

[6] Fukumoto Y. New constructional steels and structural stability. *Engineering Structures*, vol.18, pp.786-791, 1996.

[7] Ricles J. M, Sause R, Green P S. High-strength steel: implications of material and geometric characteristics on inelastic flexural behavior. *Engineering Structures*, vol.20, pp.323-335, 1998.

[8] Earls C J. Constant moment behavior of high-performance steel I-shaped beams. *Journal of Constructional Steel Research*, vol.57, pp.711-728, 2001.

[9] BS EN 1993-1-1. Eurocode 3: design of steel structures: part 1-1: general rules and rules for buildings. London: BSI; 2005.

[10] Ban H Y, Shi G, Shi Y J, et al. Research Progress on the Mechanical Property of High Strength Structural Steels. *Advanced Materials Research*, 250-253(250-253), pp.640-648, 2011.

[11] Ban H, Shi G, Shi Y, et al. Overall buckling behavior of 460 MPa high strength steel columns: Experimental investigation and design method. *Journal of Constructional Steel Research*, vol.74, pp. 140-150, 2012.

[12] Shi G, Hu F, Shi Y. Recent research advances of high strength steel structures and codification of design specification in China(J). *International Journal of Steel Structures*, vol. 14, pp. 873-887, 2014.

[13] Wang, Yan Bo, et al. "Experimental and numerical study on the behavior of axially compressed high strength steel box-columns." *Engineering Structures*, vol.58, pp.79-91, 2014.

[14] Xiong G, Kang S B, Yang B, et al. Experimental and numerical studies on lateral torsional buckling of welded Q460GJ structural steel beams(J). *Engineering Structures*, vol. 126, pp. 1-14, 2016.

[15] Yang B, Xiong G, Ding K, Nie S, Zhang W, Hu Y et al. Experimental and Numerical Studies on Lateral-Torsional Buckling of GJ Structural Steel Beams Under a Concentrated Loading Condition. *International Journal of Structural Stability and Dynamics*. 2015; 16:1640004.

[16] GB 50017-2003 Code for design of steel structures. Beijing: China Planning Press: 2003 (in Chinese).

[17] ANSI/AISC 360-10. Specification for Steel Structural Buildings. Chicago: AISC; 2010.